ADBA
Artificial Intelligence in Applied Sciences
Cutting-Edge Scientific Solutions

e-ISSN: 3108-4060
RESEARCH ARTICLE
Vol.2 / No.1 / 2026 / pp.15-26
https://doi.org/10.69882/adba.ai.2026013

Hawk-Swarmception Segmentation Network (HSCS-Net): Enhanced Liver Tumor Segmentation with Receptive Field Optimization and Clinical Data-Guided Feature Selection via PSO and GWO

Prachi Chhabra [*,1], **Sukhendra Singh** [α,2] **and Tathagat Banerjee** [β,3]

[*,α]Department of Information Technology, JSS Academy of Technical Education, Noida, [β]Department of Computer Science and Engineering, Indian Institute of Technology Patna, India.

ABSTRACT The detection and treatment of cancerous tumors in the liver are considered one of the most challenging health issues for patients globally. There is a need for fully automated systems that can precisely detect and segment the tumorous regions in medical images. This work aims to develop an automated system which utilizes a hybrid- deep- learning framework with fusion multi-scale inception feature extraction called HSCS-NET (Hawk-Swarm Ception Segmentation Network). In the proposed model, the encoder comprises of Hawk Gating with SE (squeeze-and-excitation) attention while decoders consist of adaptive attention skip fusion which comprises of Swarm ception Residual ASPP bridges. These components allow the model to recover important details of the boundaries of the tumors irrespective to their shape, size, and the tissue contrast in CT scans.In order to improve segmentation, the HSCS-NET framework is equipped with a hybrid optimization module based on PSO (Particle Swarm Optimization) and GWO (Grey Wolf Optimization) for dynamic feature selection and reliable convergence. The model was evaluated against the 3DIRCADb1 Liver Tumor Segmentation Challenge (LiTS) dataset and significantly outperformed all other models achieving a Dice coefficient value of 0.98, Accuracy of 0.9891, and Precision of 0.9901.This marks a substantial improvement over prior models such as Christ et al.'s CNN (Dice: 0.823), Wu et al.'s Fuzzy C-means + GC (Dice: 0.83), Muhammad et al.'s ResNet (Dice: 0.87, Accuracy: 0.945, Precision: 0.93), and Kaur et al.'s PSO-PSP-Net (Accuracy: 0.9754, Precision: 0.9632).The HSCS-NET architecture is mathematically grounded, modularly extensible, and validated through rigorous cross-validation and confidence refinement. With its high segmentation performance, clinical reliability, and computational efficiency, HSCS-NET stands as a superior advancement in automated liver cancer diagnostics, reducing clinician workload and improving patient prognoses through precision imaging.

KEYWORDS
Liver tumor
Segmentation
PSO
GWO
Deep learning

INTRODUCTION

Image segmentation stands as a critical computational strategy in computer vision, offering transformative potential in medical imaging and diagnostics. Among its many clinical applications, segmentation plays an instrumental role in the accurate identification and delineation of anatomical structures, which is particularly vital in oncological assessments. Liver cancer, known for its high fatality rate and diagnostic complexity, represents one of the foremost challenges in global health. It is recognized as the second most common cause of cancer-related deaths worldwide. To evaluate liver conditions and detect malignancies, radiologists primarily rely on imaging modalities such as computed tomography (CT) and magnetic resonance imaging (MRI). These modalities generate volumetric 3D scans; however, for practical implementation and computational efficiency, slice-wise 2D segmentation is often employed in both manual annotation and automated model training. Therefore, despite being

derived from 3D volumes, the use of "image segmentation" terminology is appropriate in this context. The primary methods that radiologists and oncologists traditionally use to examine liver structure and texture consist of computed tomography (CT) and magnetic resonance imaging (MRI). Multiple imaging techniques enable medical professionals to discover anomalies that function as biomarkers for liver malignancy diagnosis and ongoing observation. The combination of manual and semi-manual approaches when evaluating liver CT volume scans produces increased chances for procedural difficulties to arise. As reported by the World Health Organization, liver cancer is one of the top three causes of cancer deaths globally. Timely and precise detection of liver tumors is critical for indeed treatment and favorable prognostic outcomes. Computed Tomography (CT) imaging is

Manuscript received: 15 November 2025,
Revised: 10 December 2025,
Accepted: 12 January 2026.

[1]prachi.chhabra@gmail.com
[2]sukhendrasingh@jssaten.ac.in
[3]banerjeetathagat@gmail.com (**Corresponding author**).

instrumental in the diagnosis and staging of liver cancer. Nonetheless, the manual segmentation of the liver and the tumors associated with it from the CT images is an arduous and tedious task that is fraught with the potential for numerous errors (Cakmak *et al.* 2026). To overcome these difficulties, different automated approaches for liver and tumor segmentation have been developed, most of which emphasize the use of modern machine learning techniques in conjunction with image processing. Among these approaches, slice-wise image segmentation has been identified as an effective approach to some of the problems associated with 3D medical image segmentation. Slice-wise segmentation is the process by which a 3D volume is separated into 2D slices, each of which is then processed individually for segmentation. By converting a 3D problem into a sequence of 2D problems, this approach greatly decreases the computational burden (Pacal and Cakmak 2025).

Moreover, it permits models to consider local contextual details pertaining to each slice while also leveraging the spatial context of the full 3D volume. This has been used extensively in liver tumor segmentation since it achieves a good trade-off between computational cost and segmentation precision. The idea of slice-wise segmentation has been the subject of extensive refinement over the years, with numerous researchers contributing to this work. Christ *et al.* (2016) pioneered the use of cascaded fully convolutional neural networks (FCNs) and 3D conditional random fields (CRFs) for the automated segmentation of liver and liver lesions in CT images. Their method incorporated a cascade of FCNs to perform liver and lesion segmentation on a per-slice basis, applying CRFs to merge spatial information from neighboring slices for boundary refinement post-segmentation. This was one of the earliest works in the automation of deep learning-based liver tumor detection, demonstrating the efficacy of slice-wise segmented approaches. Many other studies have since built upon his work, demonstrating the relevance of slice-wise segmentation in clinical settings. Jin *et al.* (2020) proposed RA-UNet, a novel hybrid attention deep network aimed at extracting liver and tumor regions from CT scans.

Their approach uses an attention mechanism that helps direct the network's focus to pertinent areas in each slice, thereby increasing the accuracy of segmentation. This attention mechanism works well in CT images since the features of liver tumors are of differing intensities and textures. Slice-wise segmentation in RA-UNet helps the model to better identify the liver and tumors within each slice through parallel processing regardless of how challenging each slice may be. Jiang *et al.* (2019) also suggested AH-CNet, a hybrid deep learning model with attention and hybrid connections focused on liver tumor segmentation in CT volumes. AH-CNet processes CT images slice by slice, capturing both global and local contexts to perform the segmentation of the liver and tumors with precision. This approach allows the model to focus on specific features, such as tumor boundaries, whilst keeping in mind the inter-slice context. With the use of attention mechanisms, AH-CNet adapts to liver tumors' varying characteristics in different CT slices, improving segmentation accuracy. The past several years have witnessed great strides in the area of medical image segmentation, particularly through the use of deep learning and convolutional neural networks; CNNs, as noted by Krizhevsky *et al.* (2017) demonstrated the effectiveness of hierarchical feature learning through the use of deep CNNs for image classification. This innovation essentially caters to the progression of deep learning techniques in the domain of medical image segmentation, such as the segmentation of CT images slice-wise. Li *et al.* (2014) advanced this concept by integrating texture analysis with level-set methods for liver segmentation in CT images. Their approach utilized a multi-step method where slice-wise analysis was applied to address the challenging aspects of the liver's anatomical diversity, where texture features refined the segmentation process tailored to each slice. Li *et al.* (2018) proposed H-DenseUNet, a hybrid model of densely connected UNet tailored for liver and tumor segmentation from CT volumes. Incorporating dense connections between layers to improve feature reuse enables the model to learn complex representations, enhancing its performance. H-DenseUNet processes each CT slice independently, applying strong dense connectivity improves slice-wise segmentation accuracy and 3D CT volumetric liver tumor segmentation performance. Besides using FCNs and CNN-based approaches, the adaptive fast marching method is another approach to liver segmentation. Song *et al.* (2013) Developed a framework with an adaptive fast marching technique tailored for automatic liver segmentation in CT images, processing them slice by slice. This method is highly effective for automated liver segmentation in clinical practice because of its ability to manage a variety of complex liver shapes and heterogeneous tissue properties. The efficiency achieved through a slice-wise approach shows that each slice is processed independently, preserving accuracy while ensuring speed. Some researchers explored the use of deep learning methodologies for liver mass differentiation. Through the use of CNNs, Yasaka *et al.* (2018) classified liver masses in dynamic contrast-enhanced CT scans. Their work proved that slice-wise segmentation, where each slice was scrutinized for tumor presence, is useful for liver mass differentiation. The application of slice-wise segmentation enables the CNN to concentrate on specific features associated with each mass which enhances the model's differentiation between benign and malignant liver lesions. Liver cancer is one of the most diagnosed and deadly cancers globally; the world health organization emphasizes on this fact. In order to improve patient outcomes and lower mortality rates, early detection and accurate segmentation of liver tumors is critical (World Health Organization 2021) . Li *et al.* (2022) investigated the global burden of liver cancer and highlighted the necessity of advancements in diagnostic technologies, especially automated liver tumor segmentation systems, in order to expedite the diagnosis and treatment of the ailment. In areas that lack proficient radiologist, the application of automated segmentation techniques that use slice-wise segmentation would greatly improve the speed and precision of diagnosing liver cancer. The use of FCNs for automatic segmentation of liver tumors in multi phased contrast enhanced CT images was done by Sun *et al.* (2017). They demonstrated the successful application of slice wise segmentation in overcoming the challenges presented by multi-phase CT scans, where tumors may exhibit different appearances in each phase. Their model achieved accurate segmentation of both the liver and tumors throughout the various phases of the contrast-enhanced CT scan by processing each slice individually. In the study by Christ (2017) enhanced the understanding of convolutional neural networks in the context of medical image classification and segmentation. His approach on slice-wise segmentation, in particular, has greatly advanced the field of automated segmentation of liver and tumor tissues from CT scans. Combination of fuzzy C-means and graph cuts has proven effective for the segmentation of liver tumors in 3D CT images. Wu *et al.* (2017) applied these techniques in a slice-wise manner and achieved notable success in high accuracy segmentation. Their method is effective for complex liver tumor structures because it permits slice-by-slice tumor segmentation while maintaining spatial coherence between the slices. The work of Lu *et al.* (2020) illustrates the use of sophisticated algorithms like VGG and

extreme learning machines in the analysis of medical images. Their diagnosis of cerebral microbleeds using slice-wise segmentation displays the ability of the methodology to enhance the diagnosis and treatment strategies for many medical conditions. As has been established, slice-wise image segmentation is one of the most important techniques for liver and tumor segmentation in CT scans. Slice-wise segmentation translates 3D CT volume processing into 2D slices to lower computational workload while fully automating liver tumor segmentation. The contributions from authors such as Christ *et al.* (2016), Jin *et al.* (2020), Jiang *et al.* (2019), among others, have clearly proven the importance of deep learning and slice-wise techniques in fully automating liver tumor detection and advanced research in the domain. Given the rapid proliferation of liver cancer cases worldwide, there is an ever-growing demand for reliable and fully automated diagnostic systems, making further research into slice-wise segmentation techniques highly beneficial to liver cancer patients in regard to their treatment and prognosis.

LITERATURE REVIEW

There has been remarkable advancement in utilizing sophisticated deep learning methods for the analysis of medical images. In this review, we discuss the application of deep learning algorithms and optimization techniques in the segmentation and diagnosis of important medical disorders such as liver tumors, cerebral microbleeds, and cancers. An enhanced fuzzy C-means algorithm with graph cuts for the 3D segmentation of liver tumors in CT images marked an advancement in accurately and efficiently tumor segmenting within liver CT scans, pivotal for precision in diagnosis and treatment planning (Wu *et al.* 2017). Further study into the diagnosis of cerebral microbleeds using a VGG network with an extreme learning machine (ELM) optimized through a Gaussian map bat algorithm demonstrated the efficacy of hybrid models in enhancing diagnostic accuracy through the added complexity of microbleeds in neuroimaging (Lu *et al.* 2020). More recently, a study using MONAI and Pytorch for liver tumor segmentation in CT images highlighted the remarkable ability of transfer learning and domain-specific models to accurately identify tumors in radiological images. An optimized computer-aided diagnostic model for liver tumor detection based on InceptionV3 highlighted the need for hyperparameter optimization and model refinement in medical image analysis, especially with CT scan slices (Kaur and Kaur 2024). The ACE-SeizNet model boosts automated seizure detection through the fusion of multi-domain deep features. The integration of attention mechanisms in EEG signal processing prioritizes critical features for real-time seizure detection, demonstrating a novel application in clinical environments (Banerjee 2025a). To enhance transparency in AI models, which is pivotal for clinical validation and real-time use in cancer diagnostics, a pyramidal explainable AI framework for cervical cancer detection was proposed (Banerjee 2025b). An effective focus on diagnostic accuracy and reliability for cancer detection systems using histopathological images of lung cancer lesions was applied through a pyramidal attention network, which highlights critical tissue sample features (Banerjee 2025c). HHO-UNet-IAA, an architecture for glaucoma segmentation, employs a novel optimization-based technique which integrates attention with UNet-Inception and Harris Hawks Optimization to bolster the segmentation of glaucoma-related features in medical imaging (Banerjee *et al.* 2025). Utilizing a deep convolutional neural network, Falcon, along with transfer learning, proved effective for malaria parasite detection, showcasing the role of deep learning in disease detection with limited labeled data and pretrained models (Banerjee *et al.* 2022a). Attention mechanisms significantly improved the discrimination for detection of subtle pneumonia symptom variations, as demonstrated by the high diagnostic accuracy achieved using the attention-based discrimination model focused on mycoplasma pneumonia (Banerjee *et al.* 2022b). Further research emphasized neural network-based strategies for handling textual information highlight the significance of converting text features into vectors for machine learning in healthcare (Banerjee *et al.* 2022c). Advanced image creation strategies such as GANs are increasingly utilized within healthcare, enhancing diagnostic performance by enabling the application of deep belief convolutional networks toward pneumonia diagnoses through the augmentation of synthetic image generation techniques (Banerjee *et al.* 2021b). Integrating GANs with convolutional neural networks for improved classification of pneumonia in radiological samples demonstrates the capability of generative models to address challenges posed by limited datasets in medical imaging (Banerjee *et al.* 2021a). The study on hand sign recognition using infrared images from Leap Motion sensors contributed to novel, non-intrusive technologies in healthcare for sign language recognition aimed at aiding the hearing impaired population (Banerjee *et al.* 2021c). The application of a multi-dimensional structured neural network to analyze driving behaviors and compute a driver score advanced deep learning from the realm of healthcare to include transportation safety (Karthikeyan *et al.* 2021). The use of a single-node Hadoop cluster for small scale automation in an industrial setting illustrated the application of computational models and cluster systems in automating industrial processes, revealing the fusion of machine learning and industrial automation (Peesa *et al.* 2020). Using Resio-Inception U-Net as a thoracic organ segmentation mask enables improved segmentation of thoracic organs which aids in more precise diagnosis and treatment planning (Saminathan *et al.* 2024). An integrated method for breast cancer classification incorporating aggressiveness delineation techniques was developed which comprehensively addressed the problem of breast cancer categorization by focusing on tumor aggressiveness, a critical determinant for treatment selection (Singh *et al.* 2025a). A review post analyzing different machine learning and deep learning approaches to predicting the responses to anti-cancer drugs offered a review of approaches, which highlighted the intersection of cancer care and artificial intelligence, advancing the field of personalized medicine (Singh *et al.* 2025b). A strong prognosis model of kidney carcinoma using Swin-ViT and DeepLabV3+ with multi model transfer learning for better prognosis and characterization of the kidney carcinoma demonstrated the increasing application of transformer models and transfer learning in the analysis of medical images (Rehman *et al.* 2025). These studies highlight the significant impacts that the application of techniques of optimization and deep learning will have on medical diagnostics. It illustrates the increasing capabilities of AI in developing solutions to problems in healthcare that are more precise, more efficient, and easier to understand.

Contribution of the Study

- Study work to create a deep learning-based framework that uses varied liver tumor CT images for better region of interest identification accuracy and efficiency.
- In contrast to previous studies, which mainly depended on enhanced MRI and CT scans for narrow liver tumor type examination, this research improves feature extraction and organizational structures by employing Convolutional Neural Networks (CNNs).
- The automated system improves both diagnostic precision

and healthcare professional workflow by finding and categorizing liver tumors; therefore, it shortens the amount of time needed and work required.
- The adaptable model demonstrates the potential to develop across different inputs and circumstances, thus offering value to extended medical applications.

MATERIALS AND METHODS

Algorithm 1 Hawk-SwarmCeption Segmentation Network(HSCS-Net) presents a comprehensive and modular pipeline (showcased in Algorithm 1) designed for liver and liver tumor segmentation from CT images. The framework integrates classical image preprocessing techniques, advanced multi-scale feature extraction, attention-driven encoder-decoder design, and hybrid feature selection strategies to achieve high segmentation performance in medical imaging tasks. The pipeline starts with image preprocessing, in which each CT image is normalized by its mean and standard deviation to ensure consistency in intensity scaling across the entire dataset. After normalization, the image's contrast is enhanced using CLAHE (Contrast Limited Adaptive Histogram Equalization), which is useful in accentuating low organ contours in liver CT scans. The images are resized to a given resolution and undergo data augmentation to improve model generalization and reduce overfitting. In the multi-scale feature extraction stage, the network uses a modified version of the Inception module consisting of parallel 1×1, 3×3, and 5×5 depthwise convolutions. This model is able to capture features at different receptive fields and thus detect both fine and coarse anatomical structures. As discussed, batch normalization and ReLU activation are added after each convolutional operation to stabilize and activate the feature maps. The generated multi-scale feature maps are concatenated. They are then processed by channel attention, which adaptively adjusts the importance of each channel based on its contribution to the segmentation. Following this, the HSCS-Net is equipped with Hawk-Swarm attention-driven encoder-decoder which serves as the core structural advancement of the HSCS-Net. This module is described in Algorithm 4, which details the incorporation of Hawk gating frameworks alongside squeeze-and-excitation (SE) blocks into the encoder to improve spatial and channel feature selectivity. An Atrous Spatial Pyramid Pooling (ASPP) module is placed at the bridge between the encoder and decoder to obtain multi-scale contextual information at several dilation levels, after which Swarmception residual fusion further enhances feature representation via residual learning. The decoder employs adaptive skip fusion in which the decoder outputs are modulated with spatial attention maps and infused with the corresponding encoder features, ensuring that critical spatial details and context required for accurate segmentation are preserved. To remove limitations of the former approach, the model is augmented with a hybrid feature selection scheme which uses PSO and GWO. A binary population of feature masks is initialized representing a subset of the extracted features. In optimization, each candidate is assessed with a fitness function that combines Dice loss and Binary Cross-Entropy loss computed from the segmentation output of HSCS-Net. While PSO motivates the exploration of the feature space by updating particles with regard to personal and global best positions, GWO utilizes the social hierarchy of alpha, beta, and delta wolves to exploit the search space. The integration of both approaches facilitates and strengthens feature subset selection by minimizing redundancy and maximizing accuracy in segmentation.

The employed loss function is a weighted sum of Dice loss, Binary Cross-Entropy loss, and a structural similarity term (SSIM) which fosters overlap accuracy, pixel-wise separation fidelity, and anatomical structure preservation, respectively. Training the model with Adam optimizer applying step-wise learning rate reduction along with gradient clipping achieves stable convergence preventing explosion of the gradients during training.

Finally, the model is assessed using a comprehensive set of performance indicators including Dice coefficient, Jaccard index (IoU), Precision, Recall, and SSIM. To ensure statistical rigor, the framework implements k-fold cross validation and reports aggregated metrics such as mean, variance, and kurtosis of the performance scores across the folds. Overall, HSCS-Net framework epitomizes the integration of attention mechanisms and multi-scale feature modeling with optimization and biologically inspired reasoning, guided stratified loss functions to provide a robust, versatile, and clinically interpretable solution for liver and tumor segmentation in imaging.

Algorithm 1 Hawk-SwarmCeption Segmentation Network (HSCS-Net)

Input: Medical image dataset $\mathcal{I} = \{\mathbf{I}_1, \mathbf{I}_2, \ldots, \mathbf{I}_M\}$ with ground truth masks $\mathcal{M} = \{\mathbf{M}_1, \ldots, \mathbf{M}_M\}$

Output: Segmented masks $\mathcal{M}' = \{\mathbf{M}'_1, \ldots, \mathbf{M}'_M\}$

Step 1: Image Preprocessing
for each image $\mathbf{I}_i \in \mathcal{I}$ **do**
  Normalize: $\mathbf{I}_i \leftarrow (\mathbf{I}_i - \mu)/\sigma$
  Enhance contrast: CLAHE $\leftarrow$ CLAHE($\mathbf{I}_i$)
  Resize: $\mathbf{I}_i \leftarrow$ Resize($\mathbf{I}_i, H, W$)
  Augment: $\mathbf{I}_i \leftarrow$ Augment($\mathbf{I}_i$)
end for

Step 2: Inception-based Multi-scale Feature Extraction
for each $\mathbf{I}_i \in \mathcal{I}$ **do**
  Apply 1x1, 3x3, 5x5 depthwise convolutions
  Apply batch normalization + ReLU after each
  Concatenate features: $\mathbf{F}_i = \text{Concat}(\mathbf{F}_{1\times1}, \mathbf{F}_{3\times3}, \mathbf{F}_{5\times5})$
  Channel attention: $\mathbf{F}'_i = \text{ChannelAttention}(\mathbf{F}_i)$
end for

Step 3: Hawk-Swarm Attention-Driven Encoder-Decoder (Refer: Algorithm 4)
for each $\mathbf{F}'_i$ **do**
  Encode with SE + Hawk gating: $\mathbf{E}^i = \text{HawkGateSE}(\mathbf{F}'_i)$
  Apply ASPP: $\mathbf{B}_{ASPP} \leftarrow \text{ASPP}(\mathbf{E}^L)$
  Swarmception Residual: $\mathbf{B}_{Swarm} \leftarrow \text{SwarmRes}(\mathbf{B}_{ASPP})$
  Decode via adaptive attention skip fusion (See Algorithm 3)
  Output: $\mathbf{U}_i \leftarrow \text{Decoder}(\mathbf{B}_{Swarm}, \mathbf{E}^1, \ldots, \mathbf{E}^L)$
end for

Step 4: Hybrid Feature Selection using PSO + GWO (Refer: Algorithm 3)
Initialize binary particle population $\mathcal{X}_i^{(0)} \in \{0,1\}^n$
Fitness: Dice + BCE using $HSCS(\mathbf{I}_i, \mathcal{F}_{\mathcal{X}_i})$
for each iteration $t = 1$ to T **do**
  PSO velocity and binary update
  GWO: Compute $\mathcal{X}_1, \mathcal{X}_2, \mathcal{X}_3$ from alpha/beta/delta
  Combine: $\mathcal{X}_i^{(t+1)} = \frac{\mathcal{X}_1 + \mathcal{X}_2 + \mathcal{X}_3}{3}$
  Threshold to binary $\mathcal{X}_i^{(t+1)} \in \{0,1\}^n$
  Update fitness and bests
end for
Select optimal subset $\mathcal{F}^*$ for final segmentation

Step 5: Loss Function and Optimization
Total Loss:

$$\mathcal{L}_{\text{total}} = \lambda_1 \mathcal{L}_{\text{Dice}} + \lambda_2 \mathcal{L}_{\text{BCE}} + \lambda_3 (1 - SSIM(\mathbf{S}, \mathbf{M}))$$

Optimizer: AdamW with learning rate decay
Apply gradient clipping for training stability

Step 7: Performance Metrics and Validation
Metrics: Dice, Jaccard, Precision, Recall, SSIM via k-fold cross-validation
return Segmentation map set $\mathcal{M}'$

The Figure 1 Proposed Model framework presents a comprehensive liver segmentation pipeline utilizing deep learning and hybrid optimization techniques. It begins with image acquisition, where CT scan images are collected and split into training (70%), validation (20%), and testing (10%) subsets to ensure proper model generalization. The preprocessing stage involves image resizing, cropping, and data augmentation techniques such as rotation, flipping, and intensity variations to improve robustness. The core segmentation process is enhanced using Particle Swarm Optimization (PSO) and Grey Wolf Optimization (GWO), which optimize feature selection and hyperparameters to refine segmentation accuracy.

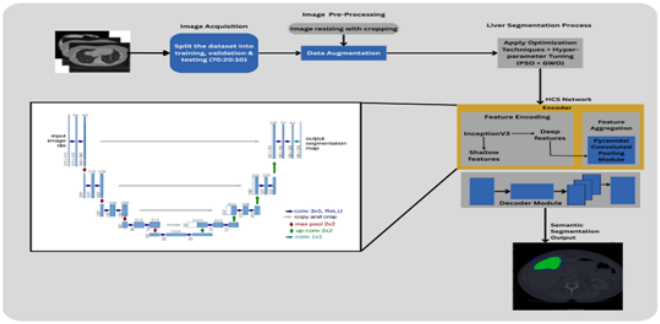

Figure 1 Proposed Model framework presents a comprehensive liver segmentation pipeline utilizing deep learning and hybrid optimization techniques

The segmentation model, referred to as HCS Network (Hybrid Convolutional Segmentation Network), utilizes an encoder-decoder structure in which the encoder performs hierarchical feature extraction and combines shallow and deep feature learning through a pyramid pooling module which enables extraction of multi- scale features. After upscaling the feature maps, the decoder incorporates skip connections to facilitate accurate boundary detection. The final output after semantic segmentation highlights the liver in green, clearly delineating it from the surrounding tissues. This framework is optimized using hybrid strategies along with multi-scale feature extraction and attention-based feature refinement to increase accuracy of segmentation, thus making it viable for medical imaging in the diagnosis of liver diseases and detection of tumors.

Data Description

The proposed approach is assessed using two datasets: 3DIRCADb1 (Bilic *et al.* 2019) and the Liver Tumor Segmentation Challenge (LiTS) (Soler *et al.* 2010). The LiTS dataset consists of abdominal CT and MRI images, with 20 sets of CT scans utilized for both training and testing purposes. Pixel-wise segmentation is conducted, with 70% of the data allocated for training, 20% for validation, and 10% for testing.

Optimization

Altering parameters for Particle Swarm Optimization (PSO) and Grey Wolf Optimization (GWO) improves the accuracy for liver tumor segmentation. PSO enhances segmentation by mimicking avian social behavior, searching for better strategies to optimize fitness loss. GWO achieves a manual balance between exploration and exploitation in pursuit of optimal segmentation results by emulating wolf hunting strategies. The novelty of utilizing these techniques lies in their ability to significantly improve the accuracy of segmentation and their flexibility in adapting to various imaging scenarios, successfully addressing challenges such as irregular tumor shapes and varying contrasts.

Hawk-Swarmception Segmentation Network

The Hawk-SwarmCeption architecture is an advanced model that merges the Encoder Decoder Module and Inception network designs by integrating cross-feature connections to enhance the efficiency of segmentation. Our combined architecture uses Encoder Decoder Module and Inception network elements to fix common problems with basic image segmentation methods (illustrated in Algorithm 2). The Encoder Decoder Module encoder-decoder design helps medical image segmentation tasks because it preserves spatial data and locates structures accurately. The network connects the encoder directly to the decoder so the feature information is protected and stays intact during the process. The Encoder Decoder Module model keeps precise anatomical information through every stage to make accurate segmentations within liver tumor areas.

Besides Encoder Decoder Module functionality, the inception network brings multi-scale feature extraction power by combining different size convolution filters into single network. The model can detect both small and large tumor details better by processing images at various levels. Parallel convolutions help the network learn context from both small and large areas which makes it better at processing different liver tumor types. The hybrid model uses combined network designs that better detects tumors while making more precise feature extractions. This design allows the network to accurately capture features of different sizes and levels of complexity, hence improving its capacity to understand a wide range of patterns and fine details inside the image. Inception modules, as observed in InceptionV3, use filters of different sizes (1x1, 3x3, 5x5) and pooling operations to achieve a comprehensive analysis of the visual features.

Algorithm 2 HSCS-NET: Liver and Liver Tumor Segmentation Algorithm

Input: CT image $\mathbf{I} \in \mathbb{R}^{H \times W}$, Ground truth label $\mathbf{L} \in \mathbb{R}^{H \times W}$
Output: Segmentation map $\mathbf{S} \in \mathbb{R}^{H \times W}$

Step 1: Input Preparation
  Load CT scan image $\mathbf{I}$
  Load corresponding ground truth mask $\mathbf{L}$

Step 2: Multi-Scale Feature Extraction via Inception Modules
for each level $i \in \{1, 2, \ldots, N\}$ **do**
  Apply Inception block: $\mathbf{F}_{\text{inc}}^{i} \leftarrow \mathcal{M}_{\text{inc}}^{i}(\mathbf{I})$
end for
Concatenate multi-scale features: $\mathbf{F}_{\text{inc}} \leftarrow \text{Concat}(\mathbf{F}_{\text{inc}}^{1}, \ldots, \mathbf{F}_{\text{inc}}^{N})$

Step 3: Cross-Feature Integration with Encoder
for each encoder layer $i \in \{1, 2, \ldots, N\}$ **do**
  $\mathbf{F}_{\text{enc}}^{i} \leftarrow \mathcal{E}^{i}(\mathbf{I})$ ▷ Extract features from encoder
  $\mathbf{F}_{\text{cross}}^{i} \leftarrow \text{Fuse}(\mathbf{F}_{\text{inc}}^{i}, \mathbf{F}_{\text{enc}}^{i})$ ▷ Cross-feature concatenation or summation
end for

Step 4: Decoding and Segmentation Reconstruction
Decode fused features using decoder: $\mathbf{S} \leftarrow \mathcal{D}(\mathbf{F}_{\text{cross}}^{1}, \ldots, \mathbf{F}_{\text{cross}}^{N})$
return S ▷ Final liver and tumor segmentation mask

Algorithm 2 HSCS-NET Network Algorithm for Liver and Liver Tumor Segmentation, showcases that the Inception modules are embedded into the Encoder Decoder Module framework, particularly within the encoder section. This integration enhances the model's feature extraction capabilities by combining detailed multi-scale features from the Inception modules with the spatial context preserved by the Encoder Decoder Module's skip connections.

Hawk-Swarm Optimization framework

The Haris-Swarm Optimization Framework presents a novel hybrid approach for feature selection by integrating two powerful swarm intelligence algorithms, Particle Swarm Optimization (PSO) and Grey Wolf Optimization (GWO) (defined in Algorithm 3). This dual-strategy mechanism is designed to identify the most relevant and informative features from a high-dimensional feature space extracted from CT scans, prior to liver and tumor segmentation using the Hawk-SwarmCeption Segmentation Network (HSCS-Net). Feature selection plays a critical role in eliminating redundancy,

reducing overfitting, and improving computational efficiency, especially in medical imaging tasks where large and complex datasets are prevalent.

As a binary vector $X_i \in \{0,1\}^n$, where each bit indicates the inclusion or exclusion of a corresponding feature. A population of such vectors is initialized randomly, forming the candidate solutions. Each solution is evaluated using a fitness function that measures segmentation performance, typically the Dice coefficient or Intersection over Union (IoU), after feeding the selected subset of features into HSCS-Net. The PSO component drives global exploration by updating each particle's velocity and position based on its personal best and the global best solution found so far. The velocity update equation incorporates inertia as well as cognitive and social terms, steering particles towards more promising areas within the search space. Following this, each particle's position is transformed into a binary vector using a sigmoid-based thresholding method.

At the same time, the GWO component captures local exploitation by simulating the social structure of grey wolves. The top three solutions which are referred to as alpha, beta, and delta are used to steer the remaining population with adaptive coefficient-based distance updates. A candidate solution is drawn towards the leading wolves, and the average of the modified positions determines where the search agent will be placed. This GWO mechanism enhances convergence by reinforcing top consensus divergence while maintaining diversity. After every iteration, both global best, which is PSO, and top wolves, GWO, are refreshed with the latest fitness score. By integrating PSO and GWO within a single framework, both the exploration and exploitation phases are optimally conducted in selecting the feature subset F^* .After selection, the subset is used as input for HSCS-Net which applies multi-scale Inception modules and cross-feature skip connections in an encoder-decoder framework to accurately segment the liver and tumors. The network's ability to disregard clinically irrelevant features enhances the accuracy and efficiency of the segmentation process and reduces the complexity of the training phase. Apart from these advantages, the Haris-Swarm architecture greatly improves the generalization capability of HSCS-Net, and simultaneously provides a robust, flexible, and scalable approach to biomedical image analysis.

Algorithm 3 introduces a biologically inspired optimization approach that combines Particle Swarm Optimization (PSO) and Grey Wolf Optimizer (GWO) to perform intelligent feature selection before final segmentation is carried out by the HSCS-Net. This hybridization ensures the selection of the most informative and discriminative features, which ultimately improves segmentation performance while reducing redundant or irrelevant data.

The pipeline begins with the initialization phase, where a population of binary solution vectors $X_i^{(0)}) \in (0,1)^n$ is generated. Each vector represents a subset of the entire feature matrix $F = f_1, f_2, \ldots, f_n$, with a '1' indicating selection and a '0' indicating exclusion of the corresponding feature. For each solution vector, the subset of features it represents is used to perform segmentation via the HSCS-Net, and the segmentation output is evaluated using performance metrics such as Dice Score or Intersection over Union (IoU). This evaluation serves as the fitness function J determining how suitable each solution is. The best-performing individual in the population is selected as the global best (GB) in the context of PSO, while the top three solutions are labelled as B_1,B_2,B_3 and are used for GWO updates, reflecting the alpha, beta, and delta wolves in the optimization hierarchy.The core of the algorithm lies in Step 1: Hybrid Optimization, where both PSO and GWO strategies are applied iteratively over a defined number of iterations T. In the PSO update, each solution adjusts its position based on its own previous best solution and the global best, incorporating random perturbations controlled by coefficients c_1 and c_2. The velocity vector is updated, and the position is transformed using a sigmoid activation function to produce a binary decision through thresholding. This ensures that the updates remain within a binary search space suitable for feature selection tasks.Concurrently, the GWO update computes new candidate solutions based on the simulated hunting behaviour of grey wolves. Distances from each of the top three wolves (B_1, B_2, B_3) to the current solution are calculated, and new positions X_1, X_2, X_3 are computed by modulating these distances with coefficients A and C, which are themselves randomly generated to simulate exploration and exploitation. The final updated position for the candidate solution is derived by averaging the three positions, and this average is again thresholder to produce a binary feature mask. The fitness of the updated solution is then reevaluated using the HSCS-Net segmentation output.After completing all iterations, the algorithm proceeds to Step 2: Feature Selection and Segmentation. Here, the best solution vector Xbest from the final iteration defines the optimal subset of features F^*. These selected features are then passed to the HSCS-Net model to generate the final segmentation output S. This step ensures that only the most relevant features, as determined by the hybrid optimization process, contribute to the segmentation, resulting in better performance and reduced computational overhead. In summary, this hybrid PSO-GWO algorithm serves as a powerful metaheuristic wrapper around the HSCS-Net segmentation model. It systematically explores the feature space to eliminate redundancy, improve segmentation accuracy, and enhance model generalization. The biologically inspired design effectively balances exploration and exploitation, yielding robust feature selection tailored to the underlying segmentation objective.

Hawk-Swarm Attention-Driven Encoder-Decoder Architecture

The Hawk-Swarm Attention-Driven Encoder-Decoder is the main framework of HSCSNet. It is aimed at improving the segmentation task by incorporating hierarchical attentionand context at multiple scales. This architecture includes three major parts: (1) Encoder with Hawk gating and SE attention paced squeeze-and-excitation (SE) attention, (2) Bridge block with Swarmception residual fusion and ASPP, and (3) Decoder with adaptive skip fusion which is highlighted in these illustrations. During the encoder phase, the input feature tensor F in $RHWC$, obtained from previous Inception modules, goes through hierarchical down-sampling through a series of strided convolutional layers. For each level I, the encoder applies a standard convolution with stride s=2 to reduce spatial dimensions and extract coarse features. These downsampled features, denoted as E^l are then refined using squeeze-and-excitation (SE) attention. The SE module computes a global descriptor z^l via global average pooling (GAP), which is subsequently transformed using a two-layer fully connected network with non-linearities (ReLU and sigmoid) to produce channel attention weights s^l. These weights recalibrate the feature maps via channel-wise scaling, allowing the network to emphasize more informative channels and suppress less relevant ones. Building upon this, a novel Hawk attention gate is introduced to perform spatial modulation. The recalibrated feature maps E^l are passed through a convolutional gating unit, where a batch normalization layer and a sigmoid activation produce a spatial gate G^l. This gate performs element-wise multiplication with the recalibrated features, resulting in spatially attentive representations $E^{(}l_{)}$. These modulated features are stored

Algorithm 3 Hybrid PSO-GWO Feature Selection Integrated with HSCS-Net for Liver and Tumor Segmentation

Input: Extracted feature matrix $\mathcal{F} = \{f_1, f_2, \ldots, f_n\}$, population size P, number of iterations T, CT image $\mathbf{I}$

Output: Final segmentation mask $\mathbf{S} \in \mathbb{R}^{H \times W}$

Initialization:

Initialize a population of binary solution vectors $\mathcal{X}_i^{(0)} \in \{0,1\}^n$ for $i = 1, 2, \ldots, P$

Each vector $\mathcal{X}_i$ encodes feature selection: $\mathcal{F}_i = \{f_j \in \mathcal{F} \mid \mathcal{X}_{i,j} = 1\}$

Evaluate the initial fitness of each particle/wolf:

$$\text{Fitness}(\mathcal{X}_i) = \mathcal{J}(HSCS(\mathbf{I}, \mathcal{F}_i)) = \text{Dice Score, IoU, etc.}$$

Identify initial global best (PSO): $\text{GB} \leftarrow \arg\max \text{Fitness}(\mathcal{X}_i)$

Identify top three wolves (GWO): $\text{B}_1, \text{B}_2, \text{B}_3 \leftarrow$ Top-3 sorted $\mathcal{X}_i$

Step 1: Hybrid Optimization via PSO and GWO

for each iteration $t = 1$ to T **do**

  for each particle/wolf $i = 1$ to P **do**

    PSO Update: Update velocity and position

$$v_i^{(t+1)} = w \cdot v_i^{(t)} + c_1 r_1 \cdot (p_i - \mathcal{X}_i^{(t)}) + c_2 r_2 \cdot (\text{GB} - \mathcal{X}_i^{(t)})$$

$$\mathcal{X}_i^{(t+1)} = \text{sigmoid}(v_i^{(t+1)}) > \theta \quad \text{(binary update)}$$

    GWO Update: Compute new position from top wolves

$$D_1 = |C_1 \cdot \text{B}_1 - \mathcal{X}_i^{(t)}|, \quad X_1 = \text{B}_1 - A_1 \cdot D_1$$

$$D_2 = |C_2 \cdot \text{B}_2 - \mathcal{X}_i^{(t)}|, \quad X_2 = \text{B}_2 - A_2 \cdot D_2$$

$$D_3 = |C_3 \cdot \text{B}_3 - \mathcal{X}_i^{(t)}|, \quad X_3 = \text{B}_3 - A_3 \cdot D_3$$

$$\mathcal{X}_i^{(t+1)} = \frac{X_1 + X_2 + X_3}{3}$$

    Threshold $\mathcal{X}_i^{(t+1)}$ to binary: $\mathcal{X}_i^{(t+1)} \in \{0,1\}^n$

    Re-evaluate fitness:

$$\text{Fitness}(\mathcal{X}_i^{(t+1)}) = \mathcal{J}(HSCS(\mathbf{I}, \mathcal{F}_i))$$

  end for

  Update personal bests and global best $\text{GB} \leftarrow \arg\max \text{Fitness}(\mathcal{X}_i)$

  Update top 3 wolves $\text{B}_1, \text{B}_2, \text{B}_3 \leftarrow \text{Sorted}(\mathcal{X}_i)$

end for

Step 2: Feature Selection and Segmentation

Extract optimal subset: $\mathcal{F}^* = \mathcal{F}_{\mathcal{X}_{\text{best}}}$

Run HSCS-Net on selected features:

$$\mathbf{S} = HSCS^{3}(\mathbf{I}, \mathcal{F}^*)$$

return S as the final segmented mask

for skip connections and forwarded through the encoder hierarchy, creating a multiscale and attention-enriched encoding.

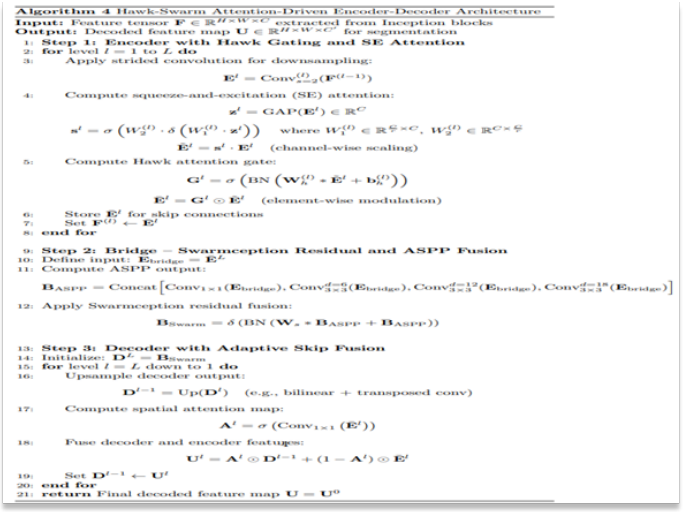

Algorithm 4 Hawk-Swarm Attention-Driven Encoder-Decoder Architecture

Input: Feature tensor $\mathbf{F} \in \mathbb{R}^{H \times W \times C}$ extracted from Inception blocks
Output: Decoded feature map $\mathbf{U} \in \mathbb{R}^{H \times W \times C'}$ for segmentation

Step 1: Encoder with Hawk Gating and SE Attention
for level $l = 1$ to L **do**
  Apply strided convolution for downsampling:

$$\mathbf{E}^l = \text{Conv}_{s=2}^{(l)}(\mathbf{F}^{(l-1)})$$

  Compute squeeze-and-excitation (SE) attention:

$$\mathbf{z}^l = \text{GAP}(\mathbf{E}^l) \in \mathbb{R}^C$$

$$\mathbf{s}^l = \sigma\left(W_2^{(l)} \cdot \delta\left(W_1^{(l)} \cdot \mathbf{z}^l\right)\right) \quad \text{where } W_1^{(l)} \in \mathbb{R}^{\frac{C}{r} \times C},\ W_2^{(l)} \in \mathbb{R}^{C \times \frac{C}{r}}$$

$$\mathbf{E}^l = \mathbf{s}^l \cdot \mathbf{E}^l \quad \text{(channel-wise scaling)}$$

  Compute Hawk attention gate:

$$\mathbf{G}^l = \sigma\left(\text{BN}\left(\mathbf{W}_h^{(l)} * \mathbf{E}^l + \mathbf{b}_h^{(l)}\right)\right)$$

$$\mathbf{E}^l = \mathbf{G}^l \odot \mathbf{E}^l \quad \text{(element-wise modulation)}$$

  Store $\mathbf{E}^l$ for skip connections
  Set $\mathbf{F}^{(l)} \leftarrow \mathbf{E}^l$
end for

Step 2: Bridge – Swarmception Residual and ASPP Fusion
Define input: $\mathbf{E}_{\text{bridge}} = \mathbf{E}^L$
Compute ASPP output:

$$\mathbf{B}_{\text{ASPP}} = \text{Concat}\left[\text{Conv}_{1\times1}(\mathbf{E}_{\text{bridge}}), \text{Conv}_{3\times3}^{d=6}(\mathbf{E}_{\text{bridge}}), \text{Conv}_{3\times3}^{d=12}(\mathbf{E}_{\text{bridge}}), \text{Conv}_{3\times3}^{d=18}(\mathbf{E}_{\text{bridge}})\right]$$

Apply Swarmception residual fusion:

$$\mathbf{B}_{\text{Swarm}} = \delta\left(\text{BN}\left(\mathbf{W}_s * \mathbf{B}_{\text{ASPP}} + \mathbf{B}_{\text{ASPP}}\right)\right)$$

Step 3: Decoder with Adaptive Skip Fusion
Initialize: $\mathbf{D}^L = \mathbf{B}_{\text{Swarm}}$
for level $l = L$ down to 1 **do**
  Upsample decoder output:

$$\mathbf{D}^{l-1} = \text{Up}(\mathbf{D}^l) \quad \text{(e.g., bilinear + transposed conv)}$$

  Compute spatial attention map:

$$\mathbf{A}^l = \sigma\left(\text{Conv}_{1\times1}\left(\mathbf{E}^l\right)\right)$$

  Fuse decoder and encoder features:

$$\mathbf{U}^l = \mathbf{A}^l \odot \mathbf{D}^{l-1} + (1 - \mathbf{A}^l) \odot \mathbf{E}^l$$

  Set $\mathbf{D}^{l-1} \leftarrow \mathbf{U}^l$
end for
return Final decoded feature map $\mathbf{U} = \mathbf{U}^0$

The bridge stage operates at the bottleneck of the encoder-decoder architecture. It begins with defining the final encoder output $E^(l_)$ as the bridge input E_bridge. The architecture then applies Atrous Spatial Pyramid Pooling (ASPP) with multiple dilation rates (6, 12, 18) to extract features at varying receptive fields, enhancing the context sensitivity of the model without increasing computation. The output from ASPP is passed through a custom Swarmception residual fusion module. This fusion block performs a residual aggregation of the ASPP features, followed by batch normalization and a ReLU activation, effectively learning deeper interactions among multiscale context representations.

In the decoder stage, the architecture initiates the reconstruction of segmentation masks from the bottleneck representation. Starting from the deepest level, the decoder performs upsampling through a combination of bilinear interpolation and transposed convolutions to increase spatial resolution. At each decoding level, the model retrieves the corresponding encoder feature $E^(l_)$ stored from the encoding phase. It computes a spatial attention map A^l using a 1×11 11×1 convolution followed by a sigmoid activation applied to the encoder feature. This attention map guides the adaptive fusion of encoder and decoder features. The final decoded feature map U^l at each level is generated as a weighted combination of decoder output and encoder features, where A^l controls the balance between new predictions and spatially rich skip features. This ensures that fine details suppressed during down-sampling are adaptively reintroduced during reconstruction.The decoder concludes by outputting the final feature map $U = U^0$, which contains the segmentation-relevant spatial and contextual information necessary to produce the final prediction. This architecture, through its combined use of SE and spatial attention (Hawk gating), context-enhancing ASPP, and adaptive skip connections, is designed to preserve structural integrity and improve boundary delineation in medical image segmentation.

The HSCS-NET network as shown by Algorithm 2 works as follows:

The Inception modules, with their diverse convolutional filters, extract rich and varied features from the input CT images. These features capture different spatial resolutions and semantic details.

Cross-Feature Connection, Features from the Inception modules are passed through cross-feature connections to the corresponding layers in Encoder Decoder Module 's decoder. This cross-connection ensures that the detailed multi-scale features are integrated with the spatial information from the encoder.

As the information from the Inception modules merges with the Encoder Decoder Module decoder, the network can utilize both high-level contextual information and fine-grained details for segmentation tasks. This hybrid approach results in more accurate and precise segmentation of liver and liver tumors.

RESULTS AND DISCUSSION

This section evaluates the quantitative and qualitative assessment of our liver segmentation method, focusing on evaluation of the measurements of Dice Coefficient, Accuracy, and Precision. The assessment of efficacy of our technique takes into account the hepatic region's division with these factors. The Dice Coefficient quantifies the overlap between prediction and actual liver region segmentation while Accuracy evaluates the over-all correctly segmented areas over the total area. Precision evaluates the segmented area counted as detected where stream of liver recognition prediction occurs while truly positive cases only comprise of a subset. All these metrics mentioned above form a composite description covering the strengths and weaknesses of our segmentation method. The training process of HSCS-Net uses systematic approaches aimed at maximum accuracy in the segmentation tasks of medical images. Image enhancement involves a series of processes starting from normalization, then resizing followed by data augmentation to increase distribution using methods such as elastic deformation, contrast adjustment, and rotation and flipping. To ensure unbiased evaluation, the dataset is divided into three equal parts comprising of training, validation, and testing in the ratio of 80:10:10. An initialization step forms a network having four encoder blocks and five decoding blocks constructed upon the Inception backbone network. A feature selection optimization strategy uses particle swarm optimization and grey wolf optimization together for maintaining discriminate spatial features during selection. Feature representation quality increases through the combination of skip connections and attention mechanisms which maintain vital information. The algorithm 4 uses dice loss together with cross-entropy loss as the training mechanism to achieve accurate segmentation and discrimination between different classes. The training utilizes Adam optimizer with 1e-4 as the initial learning rate but incorporates cosine annealing scheduling to control the learning rate dynamics across its sessions. The network performs forward propagation to generate an output that backpropagation modifies according to its weights. The algorithm stops training when the dice coefficient on validation data fails to enhance during ten successive epochs in order to avoid overfitting. The top model selection happens through validation metric assessments after which the test set receives evaluation through dice coefficient measures alongside accuracy and precision and recall and jaccard similarity metrics. HSCS-Net to effectively obtain spatial features while optimizing features and achieving the highest possible accuracy in medical image segmentation tasks.

Ablation Study

The ablation study table analyzes different model configurations by evaluating their performance through Dice Coefficient, Accuracy and Precision statistics. The different model versions use varying numbers of encoder and decoder layers as well as backbone architectures. The study investigates the impact of model depth and feature selection strategies, specifically the integration

of Particle Swarm Optimization (PSO) and Grey Wolf Optimization (GWO), on segmentation performance.

The HSCS-Net model which uses four encoder layers followed by five decoder layers obtains maximum performance results on all three metrics when coupled with the Inception backbone and PSO/GWO feature selection. The model achieves highest performance values of Dice Coefficient 0.98 and Accuracy 0.9891 combined with Precision 0.9901.

The segmentation performance decreases as the model architecture becomes shallower when using 3-encoder and 3-decoder configurations because deeper networks enable more effective spatial feature extraction and representation. A 3-encoder, 3-decoder model built with ConvexNet obtains a Dice Coefficient measurement of 0.94 however this value remains significantly lower than Dice Coefficient outcomes achieved with either 4-encoder or 5-encoder model architecture designs. The segmentation performance improves when encoder and decoder layers become deeper because deeper networks enable better identification of complex spatial patterns in the input data.

Among available backbone architectures Inception-based models show higher performance than both ResNet and ConvexNet models. The top non-Inception model combines ResNet architecture with a 4-encoder along with 5-decoder structure to reach Dice Coefficient performance at 0.96 andPrecision at 0.9793 with Accuracy at 0.9782. The performance achieved by Inception-based models surpasses other networks despite exhibiting overall measured results that are slightly weaker than the Inception pipelines. The incorporation of PSO and GWO significantly enhances performance by optimizing feature selection. This is particularly evident in models that use both optimization techniques, as they consistently outperform configurations without them. The results affirm that hybrid feature selection methods play a crucial role in refining feature extraction and improving classification robustness.

The Figure 2 visualizes the performance comparison of different model configurations based on three key metrics: Dice Coefficient, Accuracy, and Precision. The proposed HSCS-Net (4Enc-5Dec) achieves the highest scores across all three metrics, demonstrating superior segmentation performance. Inception-based architectures with Particle Swarm Optimization (PSO) and Grey Wolf Optimization (GWO) show strong results, outperforming ResNet and ConvNet variants. Notably, configurations with additional encoder and decoder layers (4Enc-4Dec and 4Enc-5Dec) tend to enhance performance, highlighting the importance of deeper architectures in improving segmentation accuracy. The plot illustrates a clear trend where hybrid optimization techniques (PSO + GWO) contribute to higher precision and robustness in segmentation.

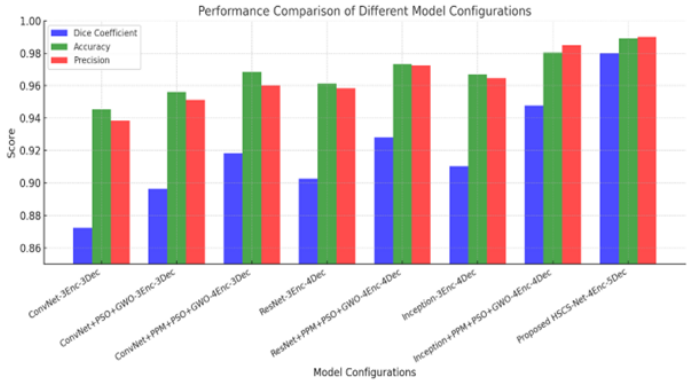

Figure 2 Ablation Study Performance

Quantitative Analysis

The performance of the proposed HSCS-NET Network in detecting liver and liver tumors from CT scan slices was assessed using confusion matrices. Figure 3 Confusion Matrix displays the confusion matrix, which highlights the detection accuracy across various liver and liver tumor scenarios within the dataset.

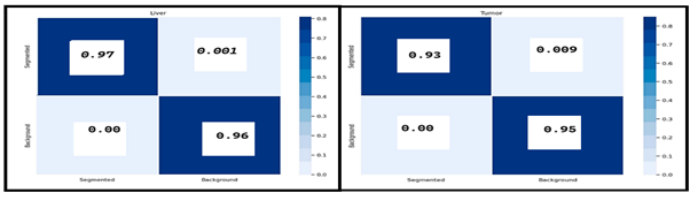

Figure 3 Confusion Matrix

In Table 2 State of the art analysis, showcases the comparison between proposed HSCS-NET Network and other state of the art techniques. The combination of high Dice Coefficient, accuracy, and precision underscores the effectiveness of the HSCS-NET Network model in liver tumor segmentation, demonstrating its ability to provide accurate and reliable diagnostic support.

Table 2 State of the art analysis

References Existing and Proposed	Dice Coefficient	Accuracy	Precision
Christ (2017) – CNN-based	0.823	–	–
Sun *et al.* (2017) – FCNs-based	–	–	–
Wu *et al.* (2017) – Fuzzy C-means & GC	0.830	–	–
Lu *et al.* (2020) – VGG & ELM	0.670	–	–
Muhammad and Zhang (2024) – ResNet	0.870	0.945	0.930
Kaur and Kaur (2024) – PSO-PSP-Net + InceptionV3	–	0.9754	0.9632
Proposed – HSCS-NET Network	0.980	0.9891	0.9901

Table 2 showcases the results of existing and proposed methods using Dice Coefficient, Accuracy and Precision. Previous CNN and/or clustering-based methods Christ (2017); Wu *et al.* (2017) achieved Dice scores around 0.82–0.83 whereas Lu *et al.* (2020) reported a Dice Coefficient of 0.67. New deep learning models perform better, including Muhammad and Zhang (2024) with a Dice score of 0.87, an accuracy of 0.945, and Kaur and Kaur (2024) achieving high accuracy (0.9754) and precision (0.9632). The developed HSCS-NET yields better results compared to all the methods and achieves 0.98 in Dice Coefficient, accuracy of 0.9891 and a specificity of 0.9772.

Table 1 HSCS-NET Ablation Study

Model Configuration	Encoder Depth	Decoder Depth	Backbone	PSO + GWO Optimization	Dice Coefficient ↑	Accuracy ↑	Precision ↑
Baseline ConvNet Segmentation	3	3	ConvexNet		0.8723	0.9452	0.9384
ConvNet + Hybrid Optimization	3	3	ConvexNet		0.8964	0.9561	0.9513
ConvNet + PPM + Hybrid Optimization	4	3	ConvexNet		0.9182	0.9685	0.9602
ResNet-based Segmentation	3	4	ResNet		0.9027	0.9613	0.9584
ResNet + PPM + Hybrid Optimization	4	4	ResNet		0.9281	0.9734	0.9725
Inception-based Segmentation	3	4	Inception		0.9104	0.9668	0.9647
Inception + PPM + Hybrid Optimization	4	4	Inception		0.9476	0.9803	0.9851
Proposed – HSCS-Net	4	5	Inception		0.9800	0.9891	0.9901

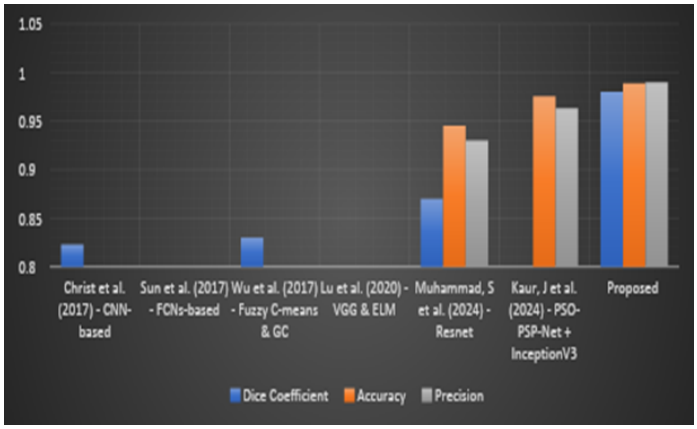

Figure 4 Comparison of our proposed model with existing state of the art methods

The graph illustrates a comparative performance analysis of existing state-of-the-art methods and the proposed HSCS-NET model based on Dice Coefficient, Accuracy, and Precision. The horizontal axis represents different methods, while the vertical axis indicates the corresponding performance scores. Earlier approaches show comparatively lower metric values, reflecting limited segmentation accuracy. Recent deep learning–based methods demonstrate noticeable improvement; however, variations in reported metrics indicate inconsistent performance across models.

The proposed HSCS-NET consistently achieves the highest values across all metrics, forming the peak of the graph. This clear performance gap highlights the effectiveness and robustness of the proposed approach over existing methods. Overall, the graphical trend confirms that HSCS-NET provides superior segmentation accuracy, precision, and reliability compared to both traditional and recent deep learning techniques.

Qualitative analysis

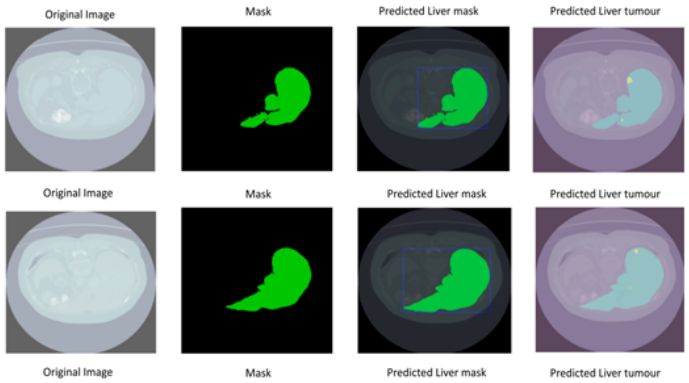

Figure 5 Liver Prediction

Figure 5 Liver Prediction demonstrates the deployment of semantic segmentation for liver and tumor lesion detection on the LiTS dataset. This figure highlights the system implementation together with its output. Semantic segmentation represents an essential medical imaging technique which divides every image pixel so healthcare specialists can distinguish healthy liver tissue from malignant lesions. The illustration shows the initial photographs alongside the generated masks used for segmenting key areas alongside model projection outputs. The masks efficiently display

the boundaries of liver tissue together with tumor locations which provides a clear visual assessment ability for both original images and segmented outputs. The illustration demonstrates how the model effectively separates distinct tissues which remains essential for doctors to make exact diagnosis and plan treatment strategies when treating liver cancer. Results from model forecasts help determine its effectiveness in operational healthcare establishments.

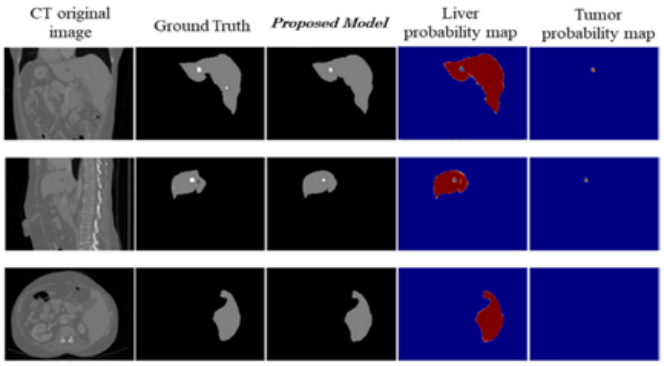

Figure 6 Liver Tumor Prediction

Dimensional Dual Path-Convolutional neural networks (TDP-CNN) together with Fully connected conditional Random fields segment both liver and tumors as shown in Figure 6 Liver Tumor Prediction. The presented segmentation outcomes display several performance outcomes. A small segment of tumor tissue shows how the model performs well for detecting restricted tumor areas and keeping them distinct. The model demonstrates its accuracy through the identification of major tumors by showing its ability to precisely retrieve substantial tumor tissues while preserving unharmed liver areas. The model demonstrates its effectiveness in intricate lesion cases through the inclusion of a sample which contains multiple tumor locations. The TDP-CNN model demonstrates reliable capabilities for detecting liver cancers accurately because of its adjustable precision in medical diagnosis and therapeutic strategy assessment.

CONCLUSION

Applying the HSCS-NET Network model achieved impressive results in terms of liver tumor detection throughput the segmentation of liver tumors achieving a Dice Coefficient of 0.98 and an accuracy of 0.9891. The model demonstrated better pixel classification than the unnamed benchmarks from other studies. The model achieved high precision performance of 0.9901 which demonstrated the model?s ability to identify tumor regions with very few misclassifications of non-tumor regions. The HSCS-NET Network demonstrated solid overall performance in both quantitative and qualitative assessments benchmarked against current state-of-the-art models. While the results with the HSCS-NET Network are encouraging, the domain adaptation problem, dataset variability, and the integration of clinical settings into the model still need additional effort. Future research in these areas could focus on creating hybrid models with domain adaptation and transfer learning techniques to improve generalization across diverse medical imaging databases. The incorporation of multiple image data types into a single system requires more efficient computing systems in order to seamlessly integrate multiple imaging data types; with this, the clinical application of CNN-based models will become more reliable. The clinical value of deep learning models as diagnostic tools for liver cancer will increase as these initiatives are undertaken.

Ethical standard

The authors have no relevant financial or non-financial interests to disclose.

Availability of data and material

The data that support the findings of this study are available from the corresponding author upon reasonable request.

Conflicts of interest

The authors declare that there is no conflict of interest regarding the publication of this paper.

Declaration of generative AI and AI-assisted technologies in the writing process

During the preparation of this work, the author(s) used artificial intelligence tools in order to improve the readability and language quality of the manuscript. After using this tool, the author(s) reviewed and edited the content as needed and take(s) full responsibility for the content of the publication.

LITERATURE CITED

Banerjee, T., 2025a Attentive CNN EEG or ACE-SeizNet: An Attention-Enhanced CNN Model for Automated EEG-Based Seizure Detection .

Banerjee, T., 2025b IMATX: An Integrated Multi-Context Pyramidal Framework for Explainable AI Predictions .

Banerjee, T., 2025c Towards Automated and Reliable Lung Cancer Detection Using DY-FSPAN. Computational Biology and Chemistry p. 108500.

Banerjee, T., D. Batta, A. Jain, S. Karthikeyan, H. Mehndiratta, *et al.*, 2021a Deep Belief CNN with GAN-Based Diagnosis of Pneumonia. In *ICEEE 2021*, Springer.

Banerjee, T., D. Butta, A. Jain, K. S. Biradar, R. R. Koripally, *et al.*, 2021b Deep Belief CNN for Diagnosis of Pneumonia. In *ICAECT 2021*, IEEE.

Banerjee, T., A. Jain, S. C. Sethuraman, S. C. Satapathy, S. Karthikeyan, *et al.*, 2022a Deep CNN (Falcon) and Transfer Learning-Based Approach to Detect Malarial Parasite. Multimedia Tools and Applications **81**: 13237–13251.

Banerjee, T., Y. F. Khan, T. Rafiq, S. Singh, R. Wason, *et al.*, 2025 HHO-UNet-IAA: Harris Hawks Optimization Based UNet Architecture for Glaucoma Segmentation. International Journal of Information Technology .

Banerjee, T., A. Sharma, K. Charvi, S. Raman, and S. Karthikeyan, 2022b Attention-Based Discrimination of Mycoplasma Pneumonia. In *ICCIDE 2021*, Springer.

Banerjee, T., A. Sharma, K. Charvi, S. Raman, R. G. Regalla, *et al.*, 2022c Journey of Letters to Vectors Through Neural Networks. In *ICDAM 2021*, Springer.

Banerjee, T., K. V. P. Srikar, S. A. Reddy, K. S. Biradar, R. R. Koripally, *et al.*, 2021c Hand Sign Recognition Using Infrared Imagery. In *ICIPTM 2021*, IEEE.

Bilic, P., P. F. Christ, E. Vorontsov, G. Chlebus, H. Chen, *et al.*, 2019 The Liver Tumor Segmentation Benchmark (LiTS). arXiv preprint arXiv:1901.04056 .

Cakmak, Y., I. Pacal, *et al.*, 2026 A comparative analysis of transformer architectures for automated lung cancer detection in ct images. Journal of Intelligent Decision Making and Information Science **3**: 528–539.

Christ, P. F., 2017 *Convolutional Neural Networks for Classification and Segmentation of Medical Images*. Ph.D. thesis, Technische Universität München, Munich, Germany.

Christ, P. F., M. E. A. Elshaer, F. Ettlinger, S. Tatavarty, M. Bickel, *et al.*, 2016 Automatic Liver and Lesion Segmentation in CT Using Cascaded Fully Convolutional Neural Networks and 3D Conditional Random Fields. In *International Conference on Medical Image Computing and Computer-Assisted Intervention (MICCAI)*, pp. 415–423, Athens, Greece, Springer.

Jiang, H., T. Shi, Z. Bai, and L. Huang, 2019 AHCNet: An Application of Attention Mechanism and Hybrid Connection for Liver Tumor Segmentation in CT Volumes. IEEE Access **7**: 24898–24909.

Jin, Q., Z. Meng, C. Sun, H. Cui, and R. Su, 2020 RA-UNet: A Hybrid Deep Attention-Aware Network to Extract Liver and Tumor in CT Scans. Frontiers in Bioengineering and Biotechnology **8**: 1471.

Karthikeyan, S., S. Gopikrishnan, D. Batta, and T. Banerjee, 2021 Double Helical Ensemble Neural Network to Analyze Driving Pattern. Turkish Journal of Computer and Mathematics Education **12**: 6447–6458.

Kaur, J. and P. Kaur, 2024 PSO-PSP-Net + InceptionV3: An Optimized Hyper-Parameter Tuned CAD Model for Liver Tumor Detection. Biomedical Signal Processing and Control **95**: 106442.

Krizhevsky, A., I. Sutskever, and G. E. Hinton, 2017 ImageNet Classification with Deep Convolutional Neural Networks. Communications of the ACM **60**: 84–90.

Li, D., L. Liu, J. Chen, H. Li, and Y. Yin, 2014 A Multistep Liver Segmentation Strategy by Combining Level Set Based Method with Texture Analysis for CT Images. In *International Conference on Orange Technologies*, pp. 109–112, Xi'an, China, IEEE.

Li, Q., M. Cao, L. Lei, F. Yang, H. Li, *et al.*, 2022 Burden of Liver Cancer: From Epidemiology to Prevention. Chinese Journal of Cancer Research **34**: 554.

Li, X., H. Chen, X. Qi, Q. Dou, C.-W. Fu, *et al.*, 2018 H-DenseUNet: Hybrid Densely Connected UNet for Liver and Tumor Segmentation from CT Volumes. IEEE Transactions on Medical Imaging **37**: 2663–2674.

Lu, S., K. Xia, and S.-H. Wang, 2020 Diagnosis of Cerebral Microbleed via VGG and Extreme Learning Machine Trained by Gaussian Map Bat Algorithm. Journal of Ambient Intelligence and Humanized Computing **14**: 5395–5406.

Muhammad, S. and J. Zhang, 2024 Segmentation of Liver Tumors by MONAI and PyTorch in CT Images with Deep Learning Techniques. Applied Sciences **14**: 5144.

Pacal, I. and Y. Cakmak, 2025 A comparative analysis of u-net-based architectures for robust segmentation of bladder cancer lesions in magnetic resonance imaging. Eurasian Journal of Medicine and Oncology **9**: 268–283.

Peesa, R. B., A. Satpathy, S. Karthikeyan, M. Bisht, T. Banerjee, *et al.*, 2020 Single Node Hadoop Cluster for Small Scale Industrial Automation. In *ICCCA 2020*, IEEE.

Rehman, A., T. Mahmood, and T. Saba, 2025 Robust Kidney Carcinoma Prognosis Using Swin-ViT and DeepLabV3+. Applied Soft Computing **170**: 112518.

Saminathan, K., T. Banerjee, D. P. Rangasamy, and M. Vimal Cruz, 2024 Segmentation of Thoracic Organs Using Resio-Inception U-Net. Current Gene Therapy **24**: 217–238.

Singh, D. P., T. Banerjee, P. Kour, D. Swain, and Y. Narayan, 2025a CICADA (UCX): Automated Breast Cancer Classification. Computational Biology and Chemistry p. 108368.

Singh, D. P., P. Kour, T. Banerjee, and D. Swain, 2025b Review of Machine Learning Models for Anti-Cancer Drug Response Prediction. Archives of Computational Methods in Engineering .

Soler, L. *et al.*, 2010 3D-IRCADb-01: A 3D Imaging Dataset of Liver Tumors. IRCAD, Strasbourg, France.

Song, X., M. Cheng, B. Wang, S. Huang, X. Huang, *et al.*, 2013 Adaptive Fast Marching Method for Automatic Liver Segmentation from CT Images. Medical Physics **40**: 091917.

Sun, C., S. Guo, H. Zhang, J. Li, M. Chen, *et al.*, 2017 Automatic Segmentation of Liver Tumors from Multiphase Contrast-Enhanced CT Images Based on FCNs. Artificial Intelligence in Medicine **83**: 58–66.

World Health Organization, 2021 Cancer. Available online.

Wu, W., S. Wu, Z. Zhou, R. Zhang, and Y. Zhang, 2017 3D Liver Tumor Segmentation in CT Images Using Improved Fuzzy C-Means and Graph Cuts. BioMed Research International p. 5207685.

Yasaka, K., H. Akai, O. Abe, and S. Kiryu, 2018 Deep Learning with Convolutional Neural Network for Differentiation of Liver Masses at Dynamic Contrast-Enhanced CT. Radiology **286**: 887–896.

How to cite this article: Chhabra, P., Singh, .S and Banerjee, T. Hawk-Swarmception Segmentation Network (HSCS-Net): Enhanced Liver Tumor Segmentation with Receptive Field Optimization and Clinical Data-Guided Feature Selection via PSO and GWO. *Artificial Intelligence in Applied Sciences*, 2(1), 15-26, 2026.